

# Evaluation of the Proposed Signal Structure for the New Civil GPS Signal at 1176.45 MHz

**June 1999**

Dr. Christopher J. Hegarty

**Sponsor:** Federal Aviation Administration  
**Dept. No.:** F082

**Contract No.:** DTFA01-93-C-00001  
**Project No.:** 02991403-03

This document has been approved for public release;  
distribution unlimited.

©1999 The MITRE Corporation

**MITRE**

**Center for Advanced Aviation System Development  
McLean, Virginia**

## **Abstract**

A signal structure for the third civil GPS signal (L5) at 1176.45 MHz has been proposed by Drs. J. J. Spilker and A. J. Van Dierendonck. This paper evaluates the performance of this signal proposal in the presence of wideband Gaussian noise (e.g., thermal noise or wideband interference) and multipath.

**KEYWORDS:** GPS, L5, third civil signal



# Table of Contents

<b>Section</b>	<b>Page</b>
<b>1. Introduction</b>	<b>1-1</b>
<b>2. Signal and Receiver Models</b>	<b>2-1</b>
2.1 Received Signals	2-1
2.2 Receiver	2-1
<b>3. Performance Evaluations</b>	<b>3-1</b>
3.1 Code Tracking Performance in Gaussian Noise	3-1
3.2 Carrier Tracking Performance in Gaussian Noise	3-3
3.3 Code Tracking Performance in Multipath	3-10
3.4 Data Demodulation	3-11
<b>4. Summary</b>	<b>4-1</b>
<b>List of References</b>	<b>RE-1</b>
<b>Glossary</b>	<b>GL-1</b>
<b>Distribution List</b>	<b>DI-1</b>

## List of Figures

<b>Figure</b>	<b>Page</b>
2-1. GPS/WAAS L5 Receiver Overview	2-2
2-2. L5 GPS/WAAS Digital Receiver Channel	2-2
3-1. Comparison of Code Tracking Accuracy Using Only Data Channel or Only Dataless Channel	3-2
3-2. Ratio of Standard Deviation of Code Tracking Error: Using Both Data and Dataless Channels vs. Using Dataless Channel Only	3-4
3-3. Simulated Code Tracking Errors Using $B_L = 1/10$ Hz	3-5
3-4. Performance of Phase Tracking Loop Implementations	3-6
3-5. I/Q Plot for Data Channel	3-8
3-6. I/Q Plot for Dataless Channel	3-8
3-7. Probability of Cycle Slip in 1-Second Interval— PLL on Dataless Channel vs. L1 C/A Code	3-9
3-8. Multipath Performance—Proposed L5	3-10
3-9. Multipath Performance of C/A Code	3-11

## Section 1

# Introduction

In [1], a detailed proposal for the design of the third civil Global Positioning System (GPS) signal is described. This proposal is based mainly on earlier work (see, e.g., [2]) of the authors of [1]. The signal proposal has also benefited significantly from input from many others, notably the “coherent carrier” concept initially proposed in [3].

This paper evaluates the performance of this signal proposal in the presence of wideband Gaussian noise (e.g., thermal noise or wideband interference) and multipath. Receiver functions that are addressed include code tracking, carrier phase tracking, and data demodulation.

The intended audience is those researchers and analysts familiar with the background leading up to the proposal for a third civil frequency and the operation of code and carrier phase tracking GPS receivers.

Section 2 presents the received signal and receiver models that were used. Section 3 derives the performance results. The paper concludes with a short summary in Section 4.

## Section 2

# Signal and Receiver Models

## 2.1 Received Signals

A simplified model for the received GPS L5 signal in the presence of thermal noise is:

$$r(t) = \sqrt{2a_1S/N_0T}c_1(t)d(t)\cos(\omega_c t + \phi) + \sqrt{2a_2S/N_0T}c_2(t)\sin(\omega_c t + \phi) + n(t) \quad (1)$$

where  $S$  is the total received power (in Watts),  $T$  is the predetection integration period (for the data channel  $T$  can be no longer than 10 ms, corresponding to one data symbol),  $N_0$  is the thermal noise power spectral density (one-sided, in Watts/Hz),  $c_1(t)$  and  $c_2(t)$  are 10.23 Mchip/s spreading waveforms,  $d(t)$  is the 100 symbol/second (50 bps data with rate  $\frac{1}{2}$  forward error correction) data waveform,  $\omega_c$  is the carrier frequency in radians/s ( $=2\pi \times 1176.45$  MHz), and  $\phi$  is the initial phase. Note that equation (1) assumes that fraction  $a_1$  of the total received power is in a data “channel,” and fraction  $a_2$  of the total received power is in a dataless “channel.” In [1],  $a_1 = a_2 = \frac{1}{2}$ . The original motivation of the dataless “channel” was to allow the use of a phase lock loop (PLL) to track carrier phase instead of requiring a Costas loop [2].

A model for the received Wide Area Augmentation System (WAAS) L5 signal is similar, except for the deletion of the dataless channel:

$$r(t) = \sqrt{2S/N_0T}c_1(t)d(t)\cos(\omega_c t + \phi) + n(t) \quad (2)$$

Also, for WAAS, the data rate is 500 symbols/second (250 bps data with rate  $\frac{1}{2}$  forward error correction) and the maximum predetection integration period is 2 ms (one data symbol).

## 2.2 Receiver

An overview of a digital receiver that could process the L5 GPS/WAAS signals is shown in Figure 2-1. Correlation with the spreading codes is performed in digital receiver channels (one per satellite being tracked). A more detailed diagram of a digital receiver channel is shown in Figure 2-2.

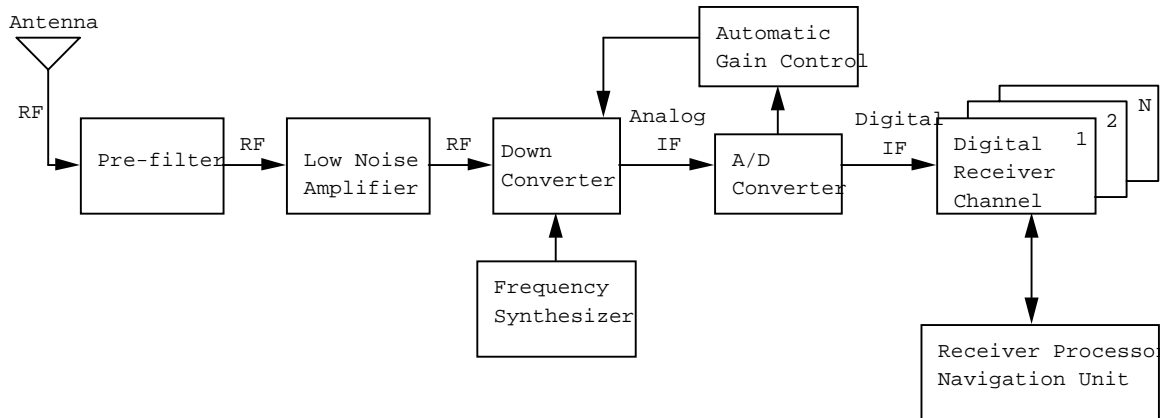


**Figure 2-1. GPS/WAAS L5 Receiver Overview**

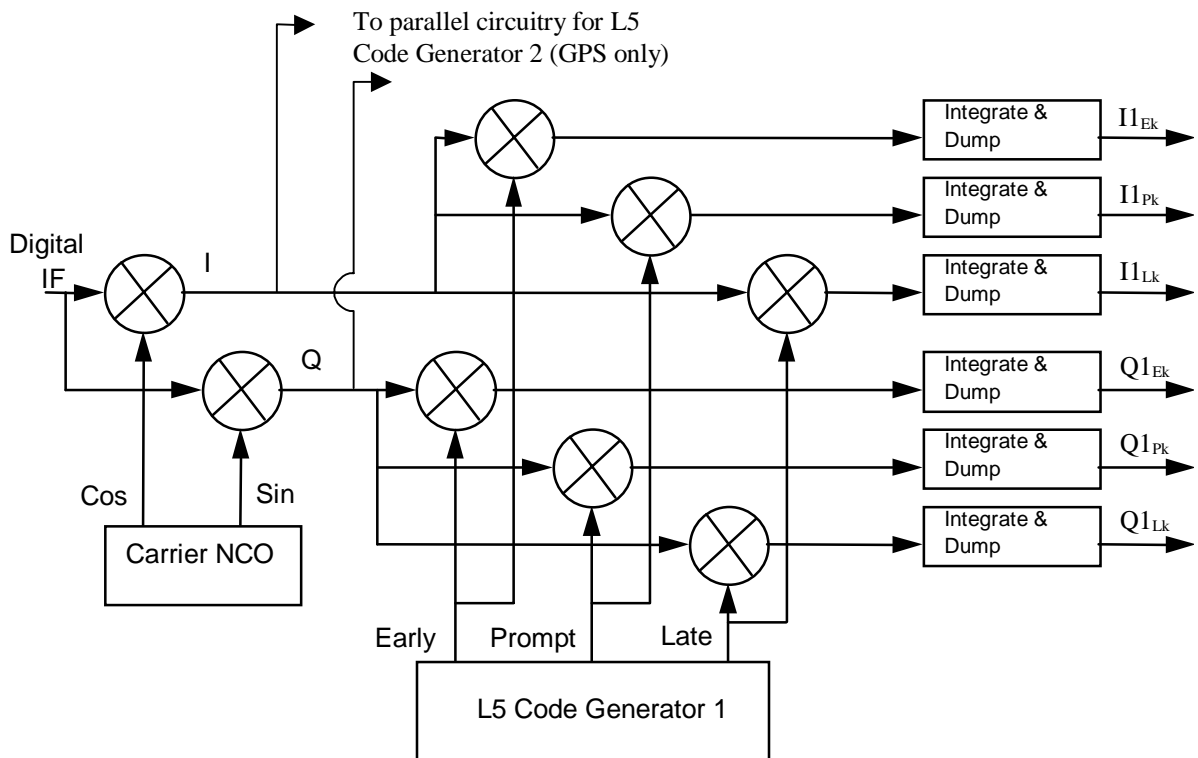


**Figure 2-2. L5 GPS/WAAS Digital Receiver Channel**

Neglecting the correlation between spreading codes, each digital receiver channel outputs may be modeled for GPS as:

$$\begin{aligned}
I_{Ek} &= \sqrt{2a_1 S / N_0 T} d_k R(\tilde{\tau} + \frac{d}{2}) \cos(\tilde{\phi}) + n_{IIEk} \\
I_{Pk} &= \sqrt{2a_1 S / N_0 T} d_k R(\tilde{\tau}) \cos(\tilde{\phi}) + n_{IIPk} \\
I_{Lk} &= \sqrt{2a_1 S / N_0 T} d_k R(\tilde{\tau} - \frac{d}{2}) \cos(\tilde{\phi}) + n_{IILk} \\
Q_{IEk} &= \sqrt{2a_1 S / N_0 T} d_k R(\tilde{\tau} + \frac{d}{2}) \sin(\tilde{\phi}) + n_{QIEk} \\
Q_{IPk} &= \sqrt{2a_1 S / N_0 T} d_k R(\tilde{\tau}) \sin(\tilde{\phi}) + n_{QIPk} \\
Q_{ILk} &= \sqrt{2a_1 S / N_0 T} d_k R(\tilde{\tau} - \frac{d}{2}) \sin(\tilde{\phi}) + n_{QILk}
\end{aligned} \tag{3}$$

And

$$\begin{aligned}
I_{2Ek} &= \sqrt{2a_2 S / N_0 T} R(\tilde{\tau} + \frac{d}{2}) \sin(\tilde{\phi}) + n_{I2Ek} \\
I_{2Pk} &= \sqrt{2a_2 S / N_0 T} R(\tilde{\tau}) \sin(\tilde{\phi}) + n_{I2Pk} \\
I_{2Lk} &= \sqrt{2a_2 S / N_0 T} R(\tilde{\tau} - \frac{d}{2}) \sin(\tilde{\phi}) + n_{I2Lk} \\
Q_{2Ek} &= \sqrt{2a_2 S / N_0 T} R(\tilde{\tau} + \frac{d}{2}) \cos(\tilde{\phi}) + n_{Q2Ek} \\
Q_{2Pk} &= \sqrt{2a_2 S / N_0 T} R(\tilde{\tau}) \cos(\tilde{\phi}) + n_{Q2Pk} \\
Q_{2Lk} &= \sqrt{2a_2 S / N_0 T} R(\tilde{\tau} - \frac{d}{2}) \cos(\tilde{\phi}) + n_{Q2Lk}
\end{aligned} \tag{4}$$

where  $d_k$  is the  $k$ -th data symbol (+1 or -1),  $\tilde{\tau} = \tau - \hat{\tau}$  is the error between the true received code phase,  $\tau$ , and the receiver's estimate of code phase,  $\hat{\tau}$ , for that channel in units of chips (one chip = 97.8 ns),  $\tilde{\phi}$  is the carrier phase tracking error,  $R(\tilde{\tau}) = 1 - |\tilde{\tau}|$  is the autocorrelation function of the spreading waveforms, and the last term of each output is noise. Since the tracking loop implementations that will be considered in the next section use the difference between the early and late correlator outputs, it is useful to define:

$$\begin{aligned}
I_{ELk} &= I_{Ek} - I_{Lk} \\
&= \sqrt{2a_1S/N_0T} \left[ R(\tilde{\tau} + \frac{d}{2}) - R(\tilde{\tau} - \frac{d}{2}) \right] \sin(\tilde{\phi}) + n_{I_{ELk}} \\
Q_{1_{ELk}} &= Q_{1_{Ek}} - Q_{1_{Lk}} \\
&= \sqrt{2a_1S/N_0T} \left[ R(\tilde{\tau} + \frac{d}{2}) - R(\tilde{\tau} - \frac{d}{2}) \right] \cos(\tilde{\phi}) + n_{Q_{1_{ELk}}}
\end{aligned} \tag{5}$$

And

$$\begin{aligned}
I_{2_{ELk}} &= I_{2_{Ek}} - I_{2_{Lk}} \\
&= \sqrt{2a_2S/N_0T} \left[ R(\tilde{\tau} + \frac{d}{2}) - R(\tilde{\tau} - \frac{d}{2}) \right] \sin(\tilde{\phi}) + n_{I_{2_{ELk}}} \\
Q_{2_{ELk}} &= Q_{2_{Ek}} - Q_{2_{Lk}} \\
&= \sqrt{2a_2S/N_0T} \left[ R(\tilde{\tau} + \frac{d}{2}) - R(\tilde{\tau} - \frac{d}{2}) \right] \cos(\tilde{\phi}) + n_{Q_{2_{ELk}}}
\end{aligned} \tag{6}$$

Importantly, with one chip spacing between the early and late correlators, and again neglecting the (low) correlation between the spreading codes used on the data and dataless channels, all noise terms on the set of outputs:

$$I_{ELk}, I_{Pk}, Q_{1_{ELk}}, Q_{1_{Pk}}, I_{2_{ELk}}, I_{2_{Pk}}, Q_{2_{ELk}}, Q_{2_{Pk}}$$

are mutually uncorrelated. The prompt outputs each have unit variance. The Early-Late outputs each have a variance equal to  $2d$  where  $d$  is the spacing (in chips) between the early and late code replicas (and, for simplicity, an infinite pre-correlation bandwidth is assumed).

## Section 3

# Performance Evaluations

### 3.1 Code Tracking Performance in Gaussian Noise

Possible code tracking loop implementations include:

1. Code tracking using just the data channel—One possible noncoherent code phase discriminator is:

$$d\tau_{1k} = \frac{I_{ELk} I_{Pk} + Q_{1ELk} Q_{1Pk}}{4a_1 S / N_0 T_1} \quad (7)$$

The variance of the code tracking error (in units of code chips squared) using this discriminator is [4]:

$$\sigma_{\tau 1}^2 = \frac{B_L}{2a_1 S / N_0} \left[ 1 + \frac{1}{a_1 S / N_0 T_1} \right] \quad (8)$$

Due to the presence of data,  $T_1$  cannot be longer than 10 ms, corresponding to one data symbol.

2. Code tracking using the dataless channel only—Similar to (7), a noncoherent discriminator that uses only the dataless channel is:

$$d\tau_{2k} = \frac{I_{2ELk} I_{2Pk} + Q_{2ELk} Q_{2Pk}}{4a_2 S / N_0 T_2} \quad (9)$$

The variance of the code tracking error (in units of code chips squared) using this discriminator has the same form as (8):

$$\sigma_{\tau 2}^2 = \frac{B_L}{2a_2 S / N_0} \left[ 1 + \frac{1}{a_2 S / N_0 T_2} \right] \quad (10)$$

However, since there is no data on this channel, the predetection integration time is no longer constrained to be less than one data symbol. The predetection integration time,  $T_2$ , may be extended to roughly the time constant of the closed tracking loop, or  $1/B_L$ . At signal-to-noise values of interest, the increased integration will eliminate the squaring loss (square bracket term in (10)), resulting in:

$$\sigma_{\tau 2}^2 \approx \frac{B_L}{2a_2 S / N_0} \quad (11)$$

For the case of equal power in the data and dataless channels (i.e.,  $a_1 = a_2 = 1/2$ ), the standard deviations of code tracking errors for the two implementations thus described are shown in Figure 3-1 with  $B_L = 1$  Hz ( $B_L$  is typically much smaller for carrier-aided implementations. However, choice of loop bandwidth does not affect the comparison).

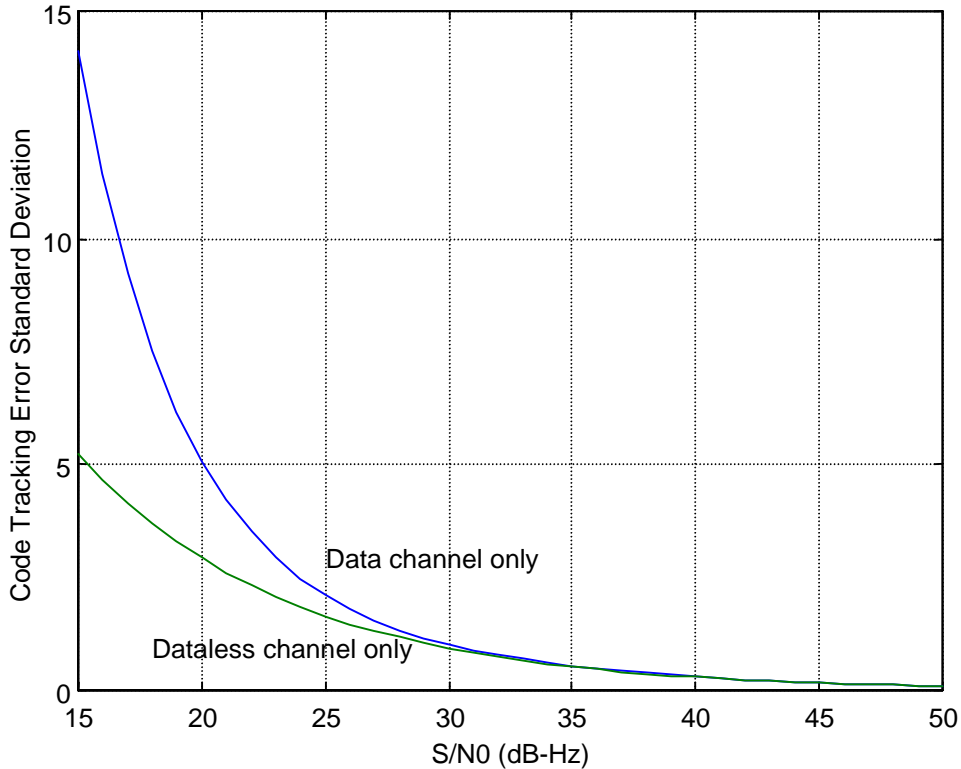


**Figure 3-1. Comparison of Code Tracking Accuracy Using Only Data Channel or Only Dataless Channel**

- Code tracking using both data and dataless channels—Improved tracking performance may be attained by utilizing both channels. A code phase discriminator that uses a linear combination of the above data channel discriminator (6) and dataless channel discriminator (7) is:

$$d\tau_k = \alpha_1 d\tau_{1k} + \alpha_2 d\tau_{2k} \quad (12)$$

where  $\alpha_1$  and  $\alpha_2$  are weighting coefficients<sup>†</sup>. So that  $d\tau_k$  provides an unbiased estimate of the code phase error, it is necessary that  $\alpha_1 + \alpha_2 = 1$ . The variance of the code tracking error (in units of code chips squared) using this discriminator is:

$$\sigma_{\tau_3}^2 = \alpha_1 \sigma_{\tau_1}^2 + \alpha_2 \sigma_{\tau_2}^2 \quad (13)$$

Of interest is the optimal choice of values for the weighting coefficients in the sense that (13) is minimized subject to the constraint  $\alpha_1 + \alpha_2 = 1$ . These optimal values are:

$$\alpha_1 = \frac{\sigma_{\tau_2}^2}{\sigma_{\tau_1}^2 + \sigma_{\tau_2}^2} \quad (14)$$

$$\alpha_2 = \frac{\sigma_{\tau_1}^2}{\sigma_{\tau_1}^2 + \sigma_{\tau_2}^2}$$

for which (13) becomes:

$$\sigma_{\tau_3}^2 = \frac{\sigma_{\tau_1}^2 \sigma_{\tau_2}^2}{\sigma_{\tau_1}^2 + \sigma_{\tau_2}^2} \quad (15)$$

Figure 3-2 illustrates the advantage in using both the data and dataless channels for code tracking by comparing the code tracking implementation of (12) with the implementation of (9). Note that for  $S/N_0$ 's above 30 dB-Hz, the standard deviation of the code tracking error due to thermal noise or wideband interference may be reduced by a factor of 70 percent ( $1/\sqrt{2}$ ) through the use of both channels. At these  $S/N_0$ 's, the optimal weighting is approximately equal between the data and dataless channels. Simulation results that validate this conclusion are shown in Figure 3-3.

In comparison with the C/A code, the new signal structure enables a reduction in RMS code tracking errors by a factor of around 3 for high signal-to-noise values. This factor is the ratio of RMS or Gabor signal bandwidths in a 24 MHz bandwidth and assumes that the optimal linear combining method described above is used.

### 3.2 Carrier Tracking Performance in Gaussian Noise

Three possible carrier loop implementations include:

1. Carrier tracking using data channel only—The Costas discriminator:

---

<sup>†</sup>Note that this description is somewhat simplified. The loop update time cannot be less than the larger of  $T_1$  and  $T_2$ . Post-detection integration must be used for  $d\tau_1$  to implement (12).

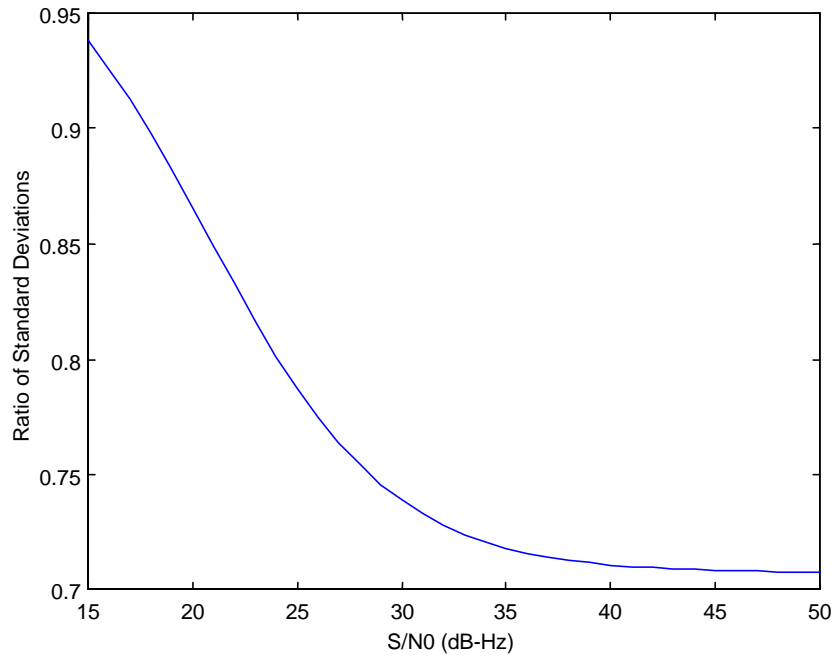


**Figure 3-2. Ratio of Standard Deviation of Code Tracking Error: Using Both Data and Dataless Channels vs. Using Dataless Channel Only**

$$d\phi_{1k} = \frac{I_{pk} Q_{1pk}}{2a_1 S / N_0 T} \quad (16)$$

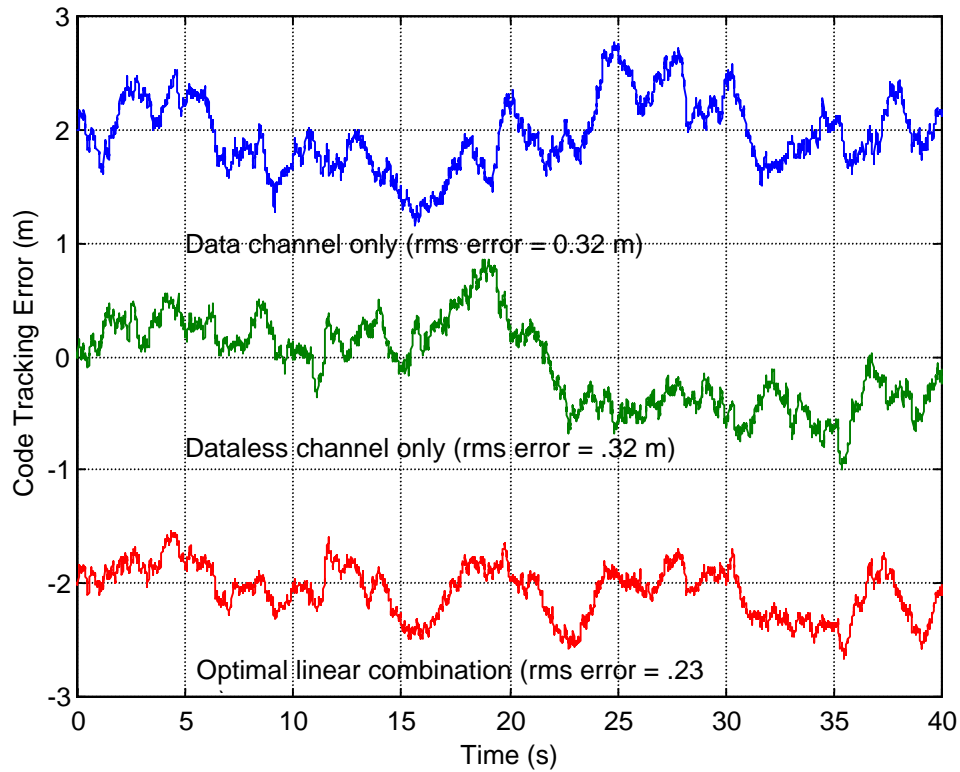
may be used resulting in a carrier phase tracking error variance (in radians squared) of:

$$\sigma_{\phi_1}^2 = \frac{B_\phi}{a_1 S / N_0} \left[ 1 + \frac{1}{2a_1 S / N_0 T_1} \right] \quad (17)$$

where  $B_\phi$  is the bandwidth (in Hz) of the closed carrier loop.

2. Carrier tracking using dataless channel only—The original motivation for the dataless channel was to permit the use of a PLL to track carrier phase only using the dataless channel. One PLL discriminator that could be used is:

$$d\phi_{2k} = \frac{I_{2pk}}{\sqrt{2a_1 S / N_0 T_2}} \quad (18)$$



Note: Each waveform has zero-mean, but was shifted on the plot to facilitate comparison.

**Figure 3-3. Simulated Code Tracking Errors Using  $B_L = 1/10$  Hz**

The variance of the carrier phase error with this implementation is:

$$\sigma_{\phi^2} = \frac{B_\phi}{a_2 S / N_0} \quad (19)$$

- Carrier tracking using both data and dataless channels—As with the code tracking loop, there appears to be some benefit in utilizing both channels for carrier phase tracking. An optimal linear combination of the data and dataless channel discriminators is given by:

$$d\phi_k = \alpha_1 d\phi_{1k} + \alpha_2 d\phi_{2k} \quad (20)$$

with weighting coefficients:

$$\alpha_1 = \frac{\sigma_{\phi_2}^2}{\sigma_{\phi_1}^2 + \sigma_{\phi_2}^2} \tag{21}$$

$$\alpha_2 = \frac{\sigma_{\phi_1}^2}{\sigma_{\phi_1}^2 + \sigma_{\phi_2}^2}$$

The carrier phase tracking variance using this discriminator is:

$$\sigma_{\phi_3}^2 = \frac{\sigma_{\phi_1}^2 \sigma_{\phi_2}^2}{\sigma_{\phi_1}^2 + \sigma_{\phi_2}^2} \tag{22}$$

Figure 3-4 compares the error standard deviations of the three carrier phase tracking methods assuming equal power in the data and dataless channels.

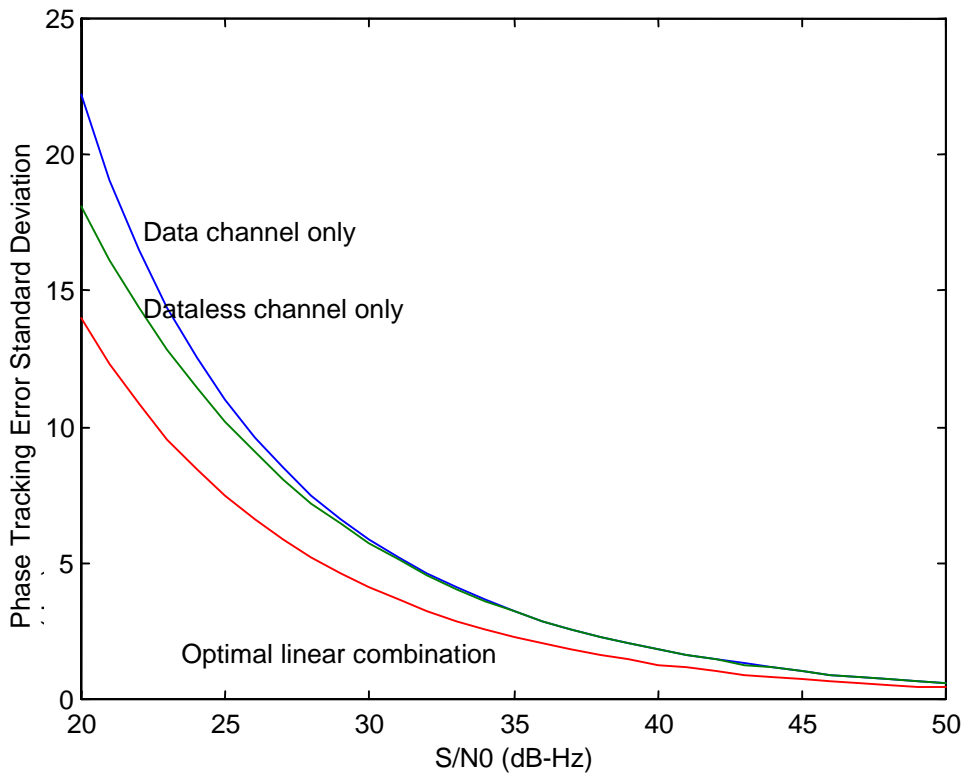


**Figure 3-4. Performance of Phase Tracking Loop Implementations**

Although some users are concerned with the magnitude of carrier phase errors (e.g., for carrier phase ambiguity resolution), most users are concerned only with maintaining carrier

phase lock so that, for example, they can continue to demodulate the data and perform carrier aiding. Thus, an important metric for these users is the  $S/N_0$  value below which reliable carrier tracking is not possible. Towards this end, the mean time between cycle slips,  $\bar{T}$ , for a first-order Costas loop may be found using [5]:

$$\bar{T} = \frac{\pi^2}{8\sigma_\phi^2 B_\phi} I_0\left(\frac{1}{4\sigma_\phi^2}\right) \quad (23)$$

for the unstressed loop case, where  $I_0$  is the zeroeth-order modified Bessel function of the first kind. For a PLL, the corresponding equation is:

$$\bar{T} = \frac{\pi^2}{2\sigma_\phi^2 B_\phi} I_0\left(\frac{1}{\sigma_\phi^2}\right) \quad (24)$$

The difference between (23) and (24) is due to the fact that the Costas loop is mathematically equivalent to a squaring loop that tracks carrier phase at *twice* the carrier frequency. This equivalence is very important, since phase tracking errors greater than 90 deg cause cycle slips with a Costas loop, whereas phase errors of up to 180 deg may be tolerated using a PLL. Figures 3-5 and 3-6 plot inphase (I) and quadrature (Q) samples of the prompt correlator output values for the data and dataless channels, respectively, when carrier phase tracking is maintained. Note from Figure 3-5 that the presence of data causes the prompt samples of the data channel correlator outputs to fall into one of two *clouds* depending on the sign of the data bit. It is impossible to distinguish amongst the noise samples between: (1) a phase tracking error greater than 90 deg, and (2) a data bit inversion. From Figure 3-6, note that only full cycle slips may occur with the dataless channel. It should be emphasized that to take full advantage of the dataless channel, a four-quadrant arctangent discriminator should be utilized on the  $I_{2Pk}$  and  $Q_{2Pk}$  samples. Although the author strongly believes that a carrier tracking implementation akin to (20) could improve cycle slip performance, this thesis has not yet been demonstrated.

The probability of a cycle slip occurring over an exposure time of  $t$  seconds is approximately:

$$P_{\text{slip}} = 1 - e^{-t/\bar{T}} \quad (25)$$

Although there are no known closed-form expressions for the slip rates of higher order loops, simulation results have indicated that higher-order loops require slightly higher values of  $S/N_0$  to achieve the performance of first-order loops. About 1 dB of additional  $S/N_0$  is required for a second-order loop [5] and roughly 2 dB more for a third-order loop (estimated from the simulation performance curves presented in [6]).

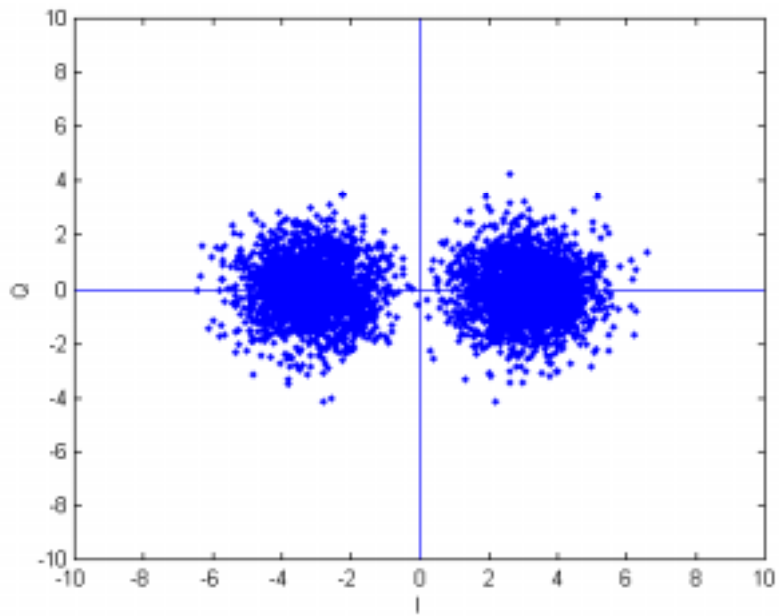


**Figure 3-5. I/Q Plot for Data Channel**

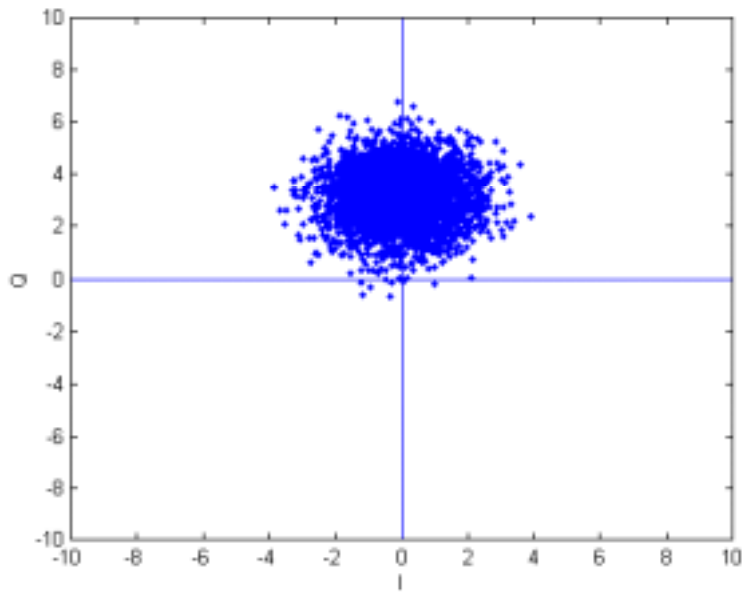


**Figure 3-6. I/Q Plot for Dataless Channel**

The probability of a cycle slip in a one-second interval for a 10 Hz PLL on the dataless channel is shown in Figure 3-7. For comparison, the probability of cycle slips for an L1 GPS receiver is shown also. Note that the coherent carrier allows robust carrier tracking at a significantly lower (3.5 dB)  $S/N_0$ . This analysis has neglected important effects such as dynamics and oscillator phase noise (see, e.g., [7]). Including these effects would degrade both curves in Figure 3-7. However, a lesser degradation would be seen in the coherent carrier curve since:

- PLL's are less sensitive to oscillator phase noise and dynamics since, as mentioned before, Costas loops mathematically track at twice the carrier frequency and thus see phase errors that are doubled.
- Because of the above, the optimal loop bandwidth of the PLL will be less than that of the Costas loop, thus suppressing the effects of Gaussian noise.

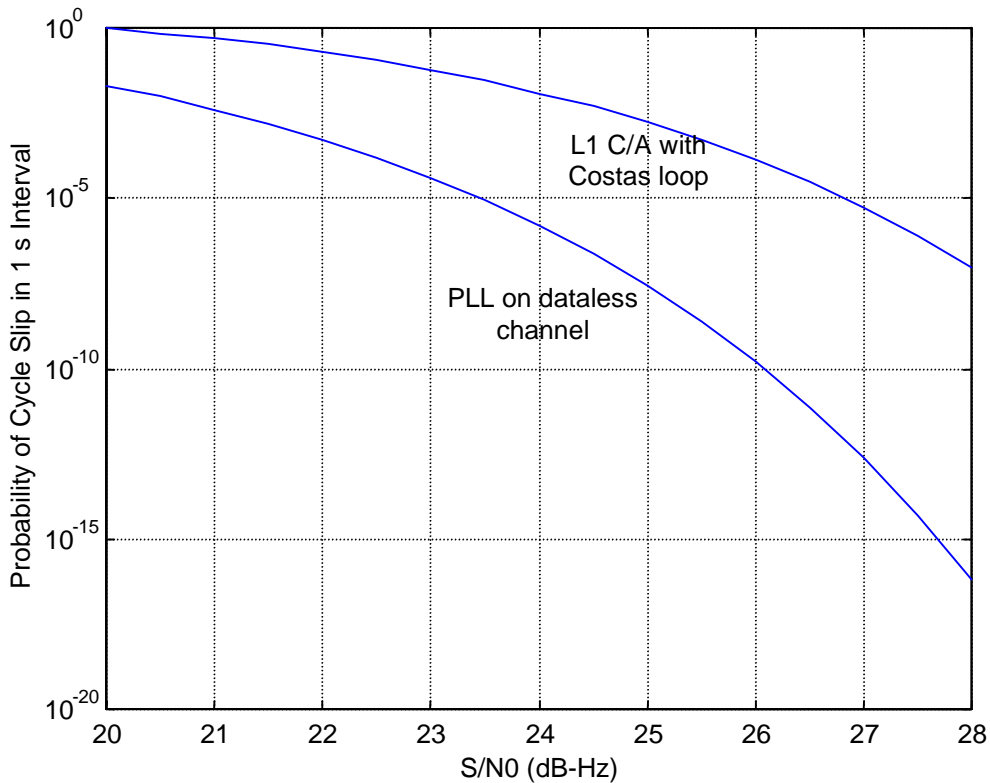


**Figure 3-7. Probability of Cycle Slip in 1-Second Interval—  
PLL on Dataless Channel vs. L1 C/A Code**

### 3.3 Code Tracking Performance in Multipath

All three code tracking discriminators described in Section 3.1 provide the same multipath performance as characterized by the maximum multipath error. Figure 3-8 shows the maximum multipath error versus multipath delay for the proposed signal structure assuming:

- A multipath signal strength of  $\frac{1}{2}$  relative to the power in the direct signal (typical values are much lower than  $\frac{1}{2}$ )
- A 24-MHz precorrelation bandwidth

The figure was produced using the method described in [8]. Although the maximum value shown in Figure 3-8 is equivalent to the maximum multipath error with the C/A code in an equivalent bandwidth (see Figure 3-9 and note the x-axis scale), the range of multipath delays causing this error are greatly reduced.

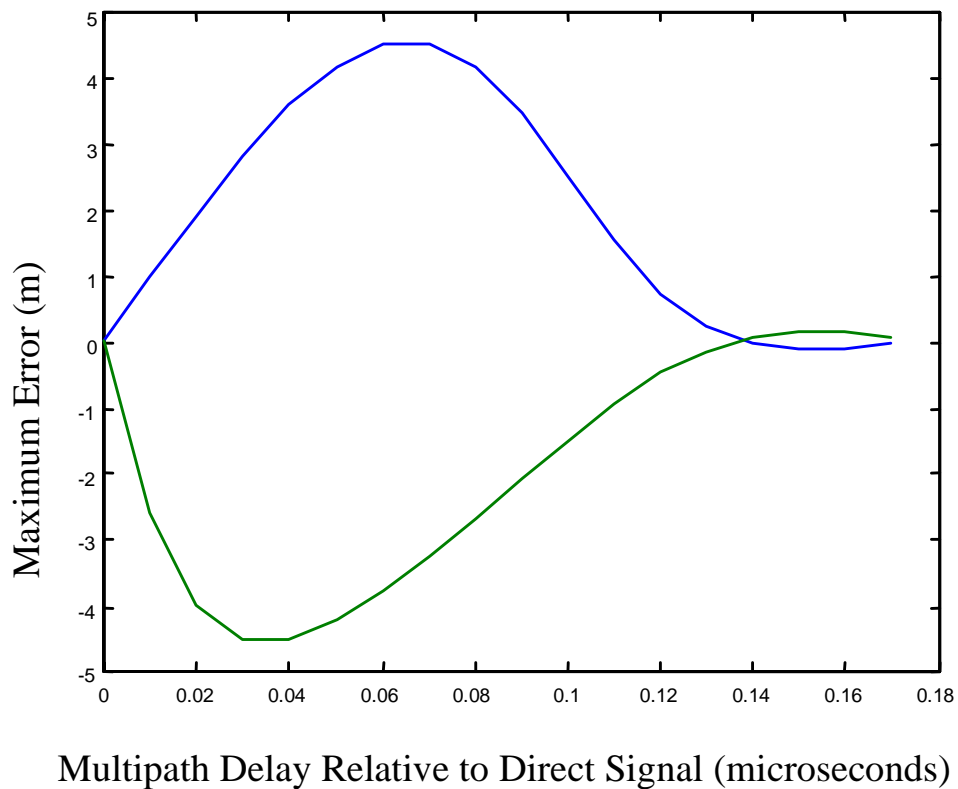


**Figure 3-8. Multipath Performance—Proposed L5**

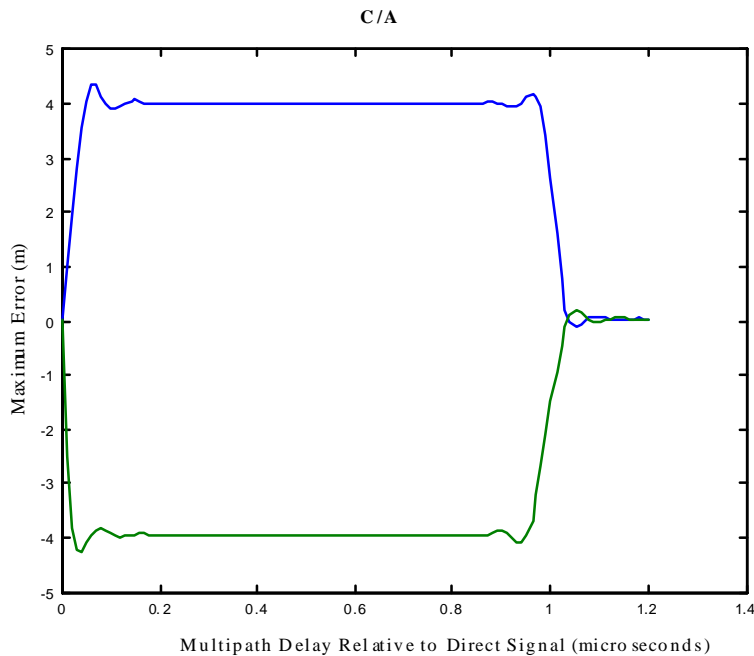


**Figure 3-9. Multipath Performance of C/A Code**

### 3.4 Data Demodulation

The division of power between the inphase and quadrature channels of the proposed signal has been a subject of debate, mainly because of two facts:

- It is well known that imperfect phase references can significantly degrade the performance of coherent data demodulation.
- Even though a PLL tracking carrier phase using just the dataless channel maintains phase lock down to much lower  $S/N_0$ 's than a Costas loop could, the phase error variance is increased because of the dedication of some of the signal power to the data channel.

The effect of the imperfect phase reference can take one of two forms:

1. If the phase errors vary slowly relative to the data symbol duration (i.e., such that the error is constant over multiple symbols), then the bit error rate is driven to the rate achieved in the presence of the worst-case phase error. For instance, if the phase error reaches a value of 50 deg ten percent of the time, then ten percent of the time data bits are being demodulated with a factor of  $\cos^2(50 \text{ deg}) = 0.4$  less bit energy than when the phase error is zero.

2. If the phase errors vary rapidly relative to the data symbol duration, then the average reduction in energy per bit for data demodulation is  $\cos^2(\sigma_\phi)$  where  $\sigma_\phi$  is the RMS phase error.

With a typical PLL bandwidth of 10 Hz, the phase errors in tracking the dataless channel will vary with a time constant on the order of 1/10 second. In comparison, the GPS data symbol duration is 10 ms (1/100 second). This observation led many, including the author, to initially believe that the effect number 1 listed above would be the appropriate one to model to determine the data demodulation performance of the proposed new signal. However, extensive Monte Carlo simulations performed by Drs. Charlie Cahn (SIRF) and Tom Morrissey (Zeta Associates) have produced results that indicate that analyzing data demodulation using effect number 2 above more closely matches simulated results. This apparent departure from theory is likely due to the memory of the forward error correction code that allows the data demodulator to “coast” through losses in signal power caused by phase tracking error excursions that can last for 10 data symbols or so.

Table 3-1 derives the  $S/N_0$  value required for a  $10^{-5}$  bit error rate assuming a 10 Hz PLL tracking the dataless channel only, using the lessons learned from the Monte Carlo simulations described above. This value is 24.8 dB-Hz. For comparison, Table 3-2 derives the  $S/N_0$  value required for the L1 C/A signal structure (phase error effects for this case are negligible and are not included in the table). The L5 structure permits robust data demodulation at a slightly lower (2 dB)  $S/N_0$  value.

**Table 3-1. Required  $S/N_0$  for  $10^{-5}$  Bit Error Rate for GPS L5**

4.5 dB	Required $E_b/N_0$ for $10^{-5}$ bit error rate
+17 dB	Conversion from bit energy to power ( $C = E_b R_b$ )
<hr/>	
= 21.5 dB-Hz	Required post-correlation $S/N_0$ in data channel
+3 dB	Ratio of total L5 signal power to power in data channel
<hr/>	
= 24.5 dB-Hz	Required post-correlation $S/N_0$ in total L5 signal with perfect phase reference
+0.3 dB	Increased $S/N_0$ required for $\cos^2(\sigma_\phi)$ reduction in signal power—see (11)
<hr/>	
= 24.8 dB-Hz	Total required post-correlation $S/N_0$

**Table 3-2. Required  $S/N_0$  for  $10^{-5}$  Bit Error Rate for GPS L1 C/A**

9.5 dB	Required $E_b/N_0$ for $10^{-5}$ bit error rate
+17 dB	Conversion from bit energy to power ( $C = E_b R_b$ )
= 26.5 dB-Hz	Required post-correlation $S/N_0$ in data channel

## Section 4

# Summary

This paper has evaluated the performance of the third civil GPS signal design proposed in [1]. The results may be summarized as follows:

- RMS code tracking errors due to thermal noise or wideband interference with the new signal structure are approximately three times lower than for the C/A code.
- The proposed code provides equivalent multipath error performance to the C/A code for short-delay multipath (signal reflections arriving less than 50 ns after the direct signal), but much better performance for longer delay multipath.
- Carrier phase tracking is much more robust for the proposed signal than for the C/A code (phase tracking is possible at a 3.5 dB lower value of  $S/N_0$ ).
- The proposed signal structure permits data demodulation at slightly lower (2 dB)  $S/N_0$  values as compared to the L1 C/A code signal structure.

In conclusion, the author has found the signal structure proposed in [1] to be an excellent design, offering significant performance improvements over the C/A code, and recommends its implementation. Several alternatives to the tracking implementations suggested in [1] are detailed in this paper and are offered to the GPS community.

## List of References

1. Spilker, J. J., and A. J. Van Dierendonck, 4 June 1999, "Signal Design for the New Civil GPS Signal at 1176.45 MHz," Revision B8.
2. Van Dierendonck, A.J., and Patrick Reddan, January 1999, "Analysis of Proposed GPS Signal Structures for Use in ARNS Bands," *Proceedings of The Institute of Navigation National Technical Meeting*, San Diego, CA.
3. Stansell, T., C. Cahn, and R. Keegan, 12 February 1999, "Lc Signal Structure," Memorandum to A.J. Van Dierendonck.
4. Van Dierendonck, A. J., 1996, "GPS Receivers," in *Global Positioning System: Theory and Applications*, B. Parkinson and J. J. Spilker, Jr., Ed., AIAA, Inc., Washington, DC.
5. Holmes, Jack K., 1990, *Coherent Spread Spectrum Communications*, Malabar, Florida: Krieger Publishing Company.
6. Stephens, S. A. and J. C. Thomas, January 1995, "Controlled-Root Formulation for Digital Phase-Locked Loops," *IEEE Transactions on Aerospace and Electronic Systems*.
7. Hegarty, C., Spring 1997, "Analytic Derivation of Maximum Tolerable In-band Interference Levels for Aviation Applications of GNSS," *NAVIGATION: Journal of The Institute of Navigation*.
8. Van Dierendonck, Fall 1992, "Theory and Performance of Narrow Correlator Spacing in a GPS Receiver," *NAVIGATION: Journal of The Institute of Navigation*.

# Glossary

**ARNS** Aeronautical Radionavigation Service

**bps** bits per second

**C/A code** coarse/acquisition code

**dB** decibel

**deg** degree(s)

**GPS** Global Positioning System

**Hz** Hertz

**MHz** Megahertz

**ms** millisecond

**ns** nanosecond

**PLL** phase lock loop

**RMS** root mean square

**S/N** signal-to-noise ratio

**WAAS** Wide Area Augmentation System

## **Distribution List**

### **Internal**

#### **F080**

R. Braff

#### **F082**

J. N. Barrer

M. B. El-Arini

J. P. Fernow

C. J. Hegarty

R. O. Lejeune

K. R. Markin

S. V. Massimini

W. A. Poor

J. K. Reagan

K. S. Sandhoo

C. A. Shively

M. J. Zeltser

F082 project file (4 copies)

F082 correspondence file (1 copy)

#### **F083**

W. Scales

#### **F084**

P. Hegarty

### **Records Resources (2)**

**DO NOT PUBLISH THIS PAGE**

**External**

Federal Aviation Administration  
800 Independence Avenue  
Washington, DC 20591

Robert N. Stanzione, AND-10

Carl McCullough, AND-730

Steve Hodges, AND-730

Robert J. Bernard (TO, Acting), ASD-10

Mike Biggs, ASR-2

Hank Cabler, AFS-430

Susan Cabler, AIR-130

Bruce DeCleene, AIR-130

Norm Fujisaki, ASD-400

Dan Hanlon, AND-730

Mike Harrison, ASD-100

Jack Loewenstein, AND-700

Brian Mahoney, AND-730

G. Markey, ASR-1

Shelley Myers, AND-1

Dave Olsen, ASD-

FAA Librarian Michelle Pate, ASD-220 (2)

D. Peterson, AND-730

B. Rovinsky, ASD-410

D. Salvano, AND-2

J. Scardina, ASD-1

Gary Skillikorn, AND-702

Ray Swider, AND-730

A. Tedford, ASD-140

